Electronic Supplementary Information

Cerium-based fluorescent nanosensor for high specific distinguishing of glutathione from cysteine and homocysteine

Tianlin Wang[a,b], Zhanhui Tao[b], Chi Qu[b], Shuo Wang[c], Yaqing Liu[a, b]*

[a] Beijing Advanced Innovation Center for Food Nutrition and Human Health, Beijing Technology and Business University, Beijing 100037, P. R. China

[b] State Key Laboratory of Food Nutrition and Safety, College of Food Engineering and Biotechnology, Tianjin University of Science and Technology, Tianjin 300457, P. R. China. Email: yaqingliu@tust.edu.cn

[c] Tianjin Key Laboratory of Food Science and Health, School of Medicine, Nankai University, Tianjin, 300071, P. R. China. Email: wangshuo@nankai.edu.cn.

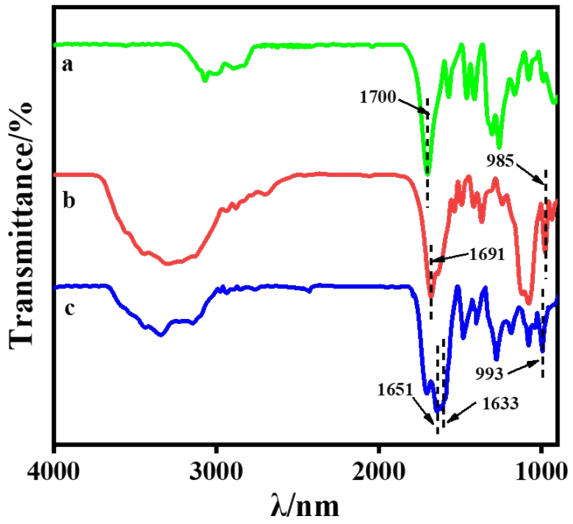

Figure S1. Fourier transfer infrared (FT-IR) spectra of DPA (curve a), GMP (curve b), and DPA-Ce-GMP (curve c).

Fourier transfer infrared (FT-IR) experiments of DPA (curve a), GMP (curve b) and DPA-Ce-GMP (curve c) were carried out to understand the assembling of DPA-Ce-GMP. The characteristic peak at 1700 cm^{-1} in DPA spectra (curve a) was assigned to the stretching vibration of -COOH group, which becomes weak in DPA-Ce-GMP spectrum (curve c). The peak at 1633 cm^{-1} in DPA-Ce-GMP spectra appeared are due to the nitrogen of pyridine that participates in the coordination with Ce. [S1-S2] The peaks at 1691 cm^{-1} and 985 cm^{-1} in GMP spectrum (curve b) are assigned to phosphate group and C=O stretching vibrations. [S3] Compared with the peaks of GMP, slight peak shifts (from 1691 cm^{-1} to 1651 cm^{-1} and from 985 cm^{-1} to 993 cm^{-1}) suggests that both phosphate and carbonyl group were involved in the coordination with Ce. [S4]

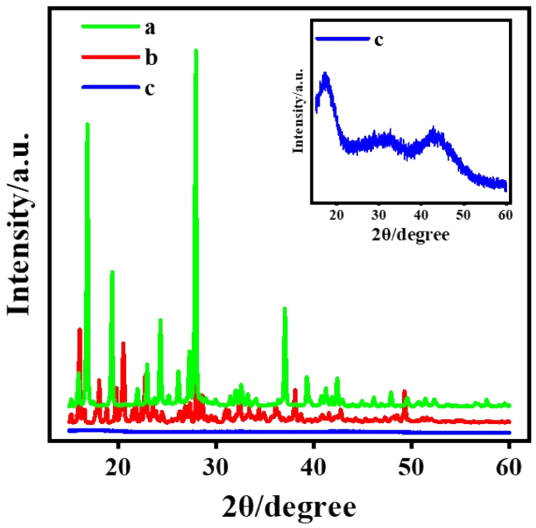

Figure S2. X-ray diffraction (XRD) spectra of DPA (a), GMP (b) and DPA-Ce-GMP (c)

X-ray diffraction (XRD) patterns of DPA (curve a) and GMP (curve b) show their typical peaks with high intensity. After forming DPA-Ce-GMP, no strong diffraction peaks are detected (curve c) since the crystallinity of DPA and GMP is destroyed after coordinating with lanthanide ions [S3].

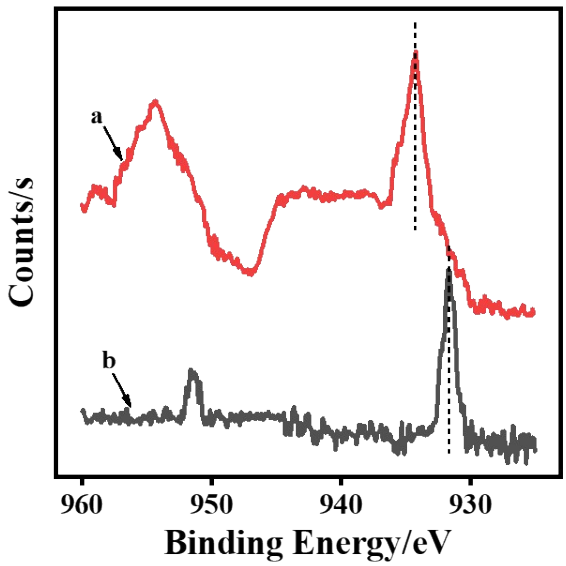

Figure S3 XPS spectra of DPA-Ce-GMP+Cu^{2+} (a), Cu-GSH (b), DPA-Ce-GMP +Cu-GSH (b).

Table S1. Comparison of different methods for GSH determination.

Method	Sensors	Linear range (μM)	Detection limit (nM)	Reference
Fluorimetry	BPMA-CQDs	0.14-13.3	42	S6
Fluorimetry	DPP-NO_2	-	61.4	S7
Fluorimetry	CDs-Br	0-34	140	S8
Fluorimetry	QDs-Cu(Ⅱ)	-	160	S9
Colorimetry	Ag(I)-TMB	0.05-8	100	S10
Colorimetry	MnO_2-MB	1-25	300	S11
Colorimetry	V_2O_5-TMB	0.01-0.5	2.4	S12
Colorimetry	CQDs-H_2O_2-TMB	0.05-20	16	S13
Fluorimetry	DPA-Ce-GMP/Cu^{2+}	0.01-40	7.1	This work

References

[S1] J. Zhao, S. Wang, S. Lu, J. Sun, X. Yang, *Nanoscale* 2018, 10, 7163-7170.

[S2] X. Chen, Y. Wang, R. Chai, Y. Xu, H. Li, B. Liu, *ACS Appl. Mater. Interfaces* 2017, 9, 13554-13563.

[S3] N. Gao, Y. Zhang, P. Huang, Z. Xiang, F. Y. Wu, L. Q. Mao, *Anal. Chem.* 2018, 90, 7004-7011.

[S4] F. Wang, X. Hu, J. Hu, Q. Peng, B. Zheng, J. Du, D. Xiao, *J. Mater. Chem. B* 2018, 6, 6008-6015.

[S5] J. Sun, B. Wang, X. Zhao, Z. Jun. Li, X. R. Yang, *Anal. Chem.* 2016, 88, 1355-

1361.

[S6] Y. Huang, J. Zhou, H. Feng, J. Zheng, H. M. Ma, W. Liu, C. Tang, H. Ao, M. Zhao, Z. Qian, *Biosens. Bioelectron*. 2016, 86, 748-755.

[S7] L. Wang, X. Chen, D. Cao, *Sens. Actuators, B* 2017, 244, 531-540.1

[S8] F. Yan, Q. Ye, J. Xu, J. He, L. Chen, X. Zhou, *Sens. Actuators, B* 2017, 251, 753-762.

[S9] Y. Hu, C. H. Heo, G. Kim, E. J. Jun, J. Yin, H. M. Kim, J. Yoon, *Anal. Chem.* 2015, 87, 3308-3313.

[S10] P. Ni, Y. Sun, H. Dai, J. Hu, S. Jiang, Y. Wang, Z. Li, *Biosens. Bioelectron.* 2015, 63, 47-52.

[S11] J. Liu, L. Meng, Z. Fei, P. J. Dyson, X. Jing, X. Liu, *Biosens. Bioelectron.* 2017, 90, 69-74.

[S12] A. B. Ganganboina, R. A. Doong, *Sens. Actuators, B* 2018, 273, 1179-1186.

[S13] Q. Zhong, Y. Chen, A. Su, Y. Wang, *Sens. Actuators, B* 2018, 273, 1098-1102.